Optimal Design Method for Surface Shape of Exterior Material to Improve Thermal Environment in Streets

Kako Futaoka[1*], *Shinji* Yoshida[2]

[1]Fujita Corporation, Sendagaya, Shibuya, Tokyo, 1510051, Japan
[2]Nara Women's University, Faculty of Human Life and Environment, Kita-uoya Nishi-machi, Nara, 6308506, Japan

Abstract. Retro-reflective materials have garnered attention as a countermeasure against heat island phenomena. However, the existing materials are inadequate for improving the thermal environment of outdoor spaces because these have been developed for traffic signs. Hence, in this study, an optimal design method for near-infrared rays retro-reflective materials to be installed on the exterior surfaces of buildings is proposed. It consists of a multi-objective genetic algorithm (MOGA) coupled with numerical analysis based on a ray tracing method. First, the outline of the method is shown. Next, the investigation of optimized surface shapes is presented. The results show that in individuals with high summer reflective performance, most of solar radiation hits a surface element only once and reflects upward in summer. In the investigation, the elevation angles of surface elements were approximately 70° and 60° for the installations in the south and west, respectively. It is predicted that the normal of the surface element where solar radiation reaches first is one of the determinants of the summer reflective performance. In addition, the effect of installation city or direction on the optimal design is analyzed. The results show that the direction does not significantly affect, the city suggests to affect the optimal design.

1 Introduction

Reducing the amount of solar radiation flowing into streets is an effective countermeasure against heat island phenomenon in summer. Hence, near-infrared rays retro-reflective materials are investigated as they can reflect the radiation to its source [1, 2]. Retro-reflective materials are made using tiny glass beads or micro corner cubes. Most existing retro-reflective materials have been developed for traffic signs. Therefore, their performance in outdoor thermal environments is insufficient. One of the reasons is their unsatisfactory retro-reflective performance when the incident angle is large [3]. This is attributable to their structure. When using retro-reflective materials as the exterior materials, a full performance is assumed not be achieved because the incident angle depends on the solar position, which changes over time. Moreover, it is sufficient enough as exterior materials to reflect toward the sky instead of strict retro-reflections. In other words, they should be designed from a perspective of thermal environment. Although studies have been conducted to develop retro-reflective material as an exterior material [4,5], the proposed designs have not been verified as optimal. In addition, the optimal design is affected by various conditions, such as the installation location and requirements. Hence, in this study, an optimal design method for near-infrared rays retro-reflective materials to be installed on the exterior surfaces of buildings is proposed. It is consisted of a multi-objective genetic algorithm (MOGA) coupled with numerical analysis based on a ray tracing method. This paper introduce a method that focuses on the surface shape and reflection properties. In addition, the effect of installation city or direction on the optimal design are discussed.

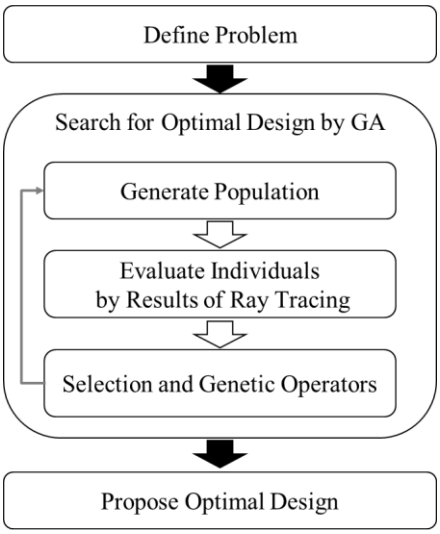

Fig. 1. The conceptual diagram of the optimal design

2 Outline of the optimal design system

2.1 System configuration

Figure 1 shows a conceptual diagram of the optimal design system proposed in this study. This system

* Corresponding author: kako.futaoka@fujita.co.jp

searches for Pareto optimal solutions by a MOGA. A computational method based on ray tracing method is applied to estimate the reflective performance [6] of each solution candidate. The reflective performance results are converted to the fitness value of each solution candidate.

2.2 Design parameters

As shown in the conceptual diagram (Fig. 2), a unit of the material surface shape comprised four reflective surfaces. In this study, the shape was referred to as a "prism." Particles of solar radiation passed through the "opening surface" ABDC and were reflected and absorbed repeatedly in the prism until they passed through the "opening surface" again. The design variables of the prism are listed in Table 1, and the definitions of the variables are shown in Fig. 2.

2.3 Design goals and objective functions

For the MOGA, a design goal must be established and the achievement degree (fitness) of the goal for each candidate solution (individual) must be evaluated. In the present study, we defined three design goals: (1) high retro-reflectivity to solar radiation in summer, (2) high absorption rate of prism itself or streets in winter and (3) a simple shape that can be easily arranged cyclically.

Furthermore, we defined objective functions to evaluate the fitness of each goal. The values of the fitness ranged from 0 to 1, where higher values indicated better fitness states. The symbols used in the functions in this study are summarized in Table 2.

(1) Summer reflective performance: F_{Summer}

F_{Summer} is a function used to evaluate the contribution to the heat load reduction in a street canyon in summer (Equations 1-1 and 1-2).

$$F_{Summer} = J_{up} / J_{dv} \tag{1-1}$$

$$J_{up} = \Sigma[i=1,m]\{\rho_i \cdot max(sin\theta_i, 0)\} \tag{1-2}$$

When solar radiation reaches the prism surface, it is either absorbed or reflected (Fig. 3). The reflected component is categorized based on whether its vector is upward or downward. Upward reflection contributes positively to the thermal environment in summer because solar radiation does not remain in the street canyon but returns to the sky. Moreover, the larger θ_i, the elevation angle of reflection vector, the lower is the probability of the solar radiation reaching the other building wall in the streets. Therefore, the intensity of each reflection vector is weighted by $sin\theta_i$.

Table 1. The design variables of the prism

Variable	Definition	Range
X_1	Type(refer to Fig. 2)	$0 \leqq X_1 \leqq 1$
X_2	Aspect of opening surface	$0.01 \leqq X_2 \leqq 1.00$
X_3	Angle between Z-axis and AB	$-80^\circ \leqq X_3 \leqq 80^\circ$
X_4	Vertex E	$0.01 \leqq X_4 \leqq 1.00$
X_5		$0 \leqq X_5 \leqq 1.00$
X_6		$0 \leqq X_6 \leqq 1.00$
X_7	Vertex F	$0 \leqq X_7 \leqq 1.00$
X_8	Rotation angle of prism	$0^\circ \leqq X_8 \leqq 175^\circ$

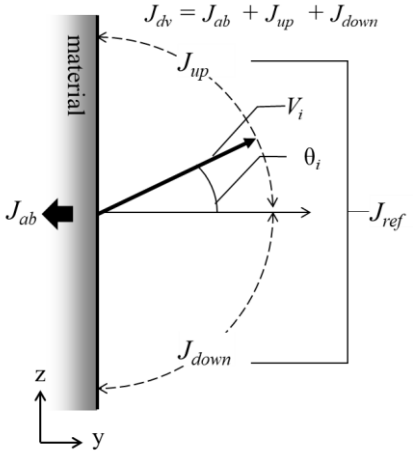

Fig. 3. The diagram of reflection and absorption

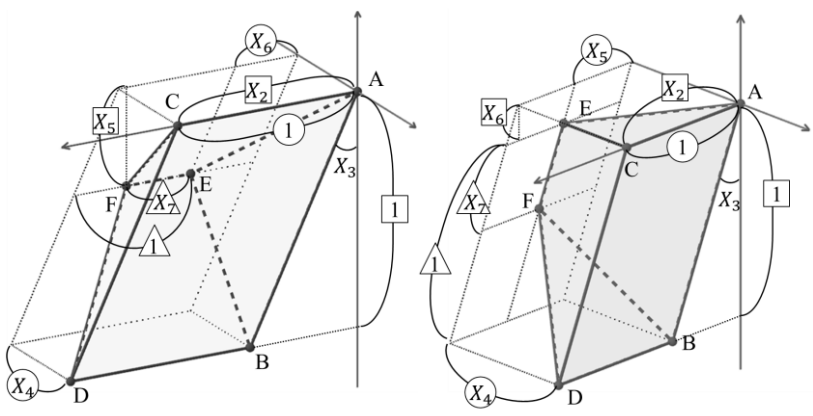

(a) Type=1 (b) Type=1

Fig. 2. The conceptual diagram of prism

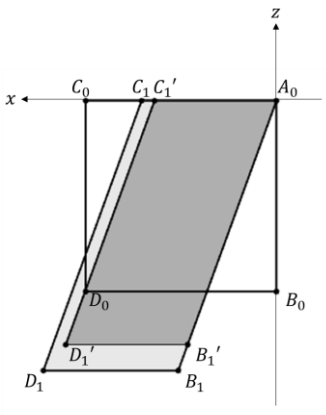

Fig. 4. The conceptual diagram of reflection and absorption

(2) Winter reflective performance: F_{Winter}

F_{Winter} is defined in Equation 2-1 and is applied to evaluate absorption and downward reflection.

$$F_{Winter} = (J_{ab} + 0.8 \cdot J_{down}) / J_{dv} \quad (2\text{-}1)$$

In winter, the thermal environment is more suitable for people when more solar radiation is absorbed by the prisms or flows into streets. In this function, the mean absorption rate of the streets is assumed to be 0.8, and reflection is considered once in the streets.

(3) Evaluation of opening surface: F_{Form}

In the present analysis, the fitness of the prism shape was evaluated from its opening surface. It is expressed as the ratio of cross product (Equations 3-1).The definitions of the symbols are provided in Fig. 4.

$$F_{Form} = |\boldsymbol{A_0B_1'} \times \boldsymbol{A_0C_1'}| / |\boldsymbol{A_0B_0} \times \boldsymbol{A_0C_0}| \quad (3\text{-}1)$$

$\boldsymbol{A_0B_1}$ and $\boldsymbol{A_0C_1}$ satisfy the following conditions.
- Parallelogram $A_0B_1C_1D_1$ is an opening surface of prism.
- The areas of parallelograms $A_0B_0C_0D_0$ and $A_0B_1C_1D_1$ are equal.
- Parallelograms $A_0B_1C_1D_1$ and $A_0B_1'C_1'D_1'$ are similar.
- Parallelograms $A_0B_0C_0D_0$ and $A_0B_1'C_1'D_1'$ have the same perimeter.

Although manufacturing cost is not considered in this study, obtaining only unrealistic shapes as optimal solutions is undesirable. In this function, the best form of the opening surface is a square, and the greater the deviation from this shape, the worse is the evaluation.

3 Effect of Installation location on optimal shape

3.1 Purpose of analysis

The reflection properties at a certain time depend on the relationship between the prism shape and the incidence angle. In other words, the optimal shape is considered to be affected by the surface direction or installation of cities. Therefore, two parameters, i.e., the locations of cities and the direction of the vertical surface were focused and their effects on the optimal design were analyzed.

3.2 Methods

In this study, parametric studies were conducted. The computational cases are summarized in Table 3. Osaka (34.68 °N, 135.52 °E) and Hong Kong (22.31 °N, 114.00 °E) were selected as the survey cities. Both cities are significantly affected by heat island phenomena. In summer, the temperatures of these cities reach the maximum at approximately 3 p.m. Fig. 5 shows the trajectories of the sun in those cities at the target dates. The vertical axis indicates the altitude of the sun,

Table 2. Symbols in the functions

F_{Summer}	: Reflective performance in summer [-]
F_{Winter}	: Reflective performance in winter [-]
F_{Form}	: the evaluation of opening surface [-]
J_{up}	: Amount of reflected solar radiation directed upward [W/㎡]
J_{down}	: Amount of reflected solar radiation directed downward [W/㎡]
J_{ref}	: Amount of reflected solar radiation [W/㎡]
J_{ab}	: Amount of solar radiation absorbed by a prism [W/㎡]
J_{dv}	: Amount of incident solar radiation [W/㎡]
ρ_i	: Reflection intensity of vector V_i [-]
α	: Absorption rate of prism [-]
V_i	: Reflection vector
m	: Number of types of reflection vector
θ_i	: Elevation angle of reflection vector V_i [°]

Table 3. Analysis case

Case	City	Direction	Analysis Target	
			Date	Time ※1)
1	Osaka	South	21/06/2020 21/08/2020	10a.m. 12p.m. 2p.m.
2	Osaka	West	21/12/2020 21/02/2021	1p.m., 3p.m.
3	Hong Kong	West		

※1) local time

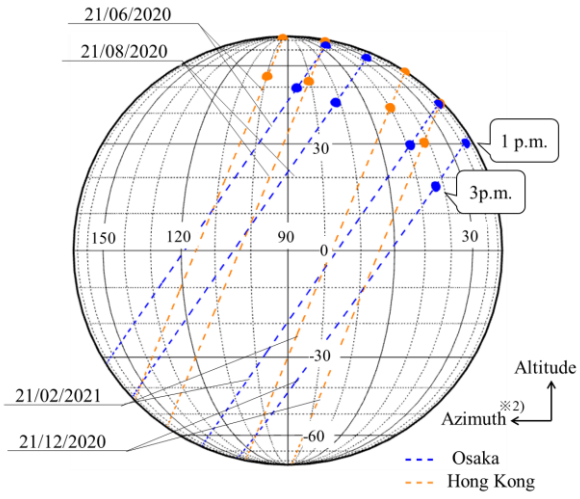

※2) Azimuth: east = -90°, south = 0°, west = +90°

Fig. 5. The sun path of target dates

Table 4. The setting of MOGA

Population	48
Generation	60
Selection	Pareto reservation strategy [7]
Crossover rate	0.9
Mutation rate	0.01

whereas the horizontal axis indicates the azimuth. The blue dashed lines indicate the sun paths for Osaka, whereas the orange lines those for Hong Kong. The circles on the dashed lines also indicate the solar positions at the target time in the present analysis. The solar positions for each site at the target date were calculated by the following equations based on spherical trigonometry:

$$\sin h = \sin\varphi \cdot \sin\delta + \cos\varphi \cdot \cos\delta \cdot \cos t \quad (1)$$

$$\sin A = ((\cos\delta \cdot \sin t)) / \cos\varphi \quad (2)$$

$$\cos A = ((\sin h \cdot \sin\varphi - \sin\delta)) / ((\cos h \cdot \cos\varphi)) \quad (3)$$

where h is the solar altitude, and A is the solar azimuth. The symbols φ, δ, and t denote the latitude of the site, the declination of the sun, and the hour angle. The sun paths of these cities are different owing to their locations. In particular, in the afternoon of June 21, 2020, the azimuth of the sun shifted from 0° to +120° in Osaka and from 95° to 100° in Hong Kong.

The south and west directions were selected as the facing directions of the vertical surfaces. The sun path shows a parabola with a vertex at approximately noon in the case of the south surface. On the other hand, the sun altitude decreased as time progressed in the west.

Four target dates were selected for analysis. June 21, 2020 (the summer solstice) and August 21, 2020 dates were selected as the summer dates, whereas December 21,2020 (the winter solstice) and February 21,2021 as the winter dates. The target times were set to 10 a.m., 12 p.m., and 2 p.m. for Case 1 (the surface facing the southern direction), and 1 p.m. and 3 p.m. for Cases 2 and 3 (the surface facing the western direction).

The MOGA settings are listed in Table 4. In the present analysis, the population in a generation was set to 48, and 60 generations, or 2880 samples were evaluated. The reflection properties were estimated by ray tracing method, which considers only specular reflection, assuming that the surface elements of a prism are ideal specular surfaces with a reflectance of 0.9. Because no single solution ordinary exists in a multi-objective optimization problem, designers must make a decision to select the most preferred solution.

Our main aim in this study is to develop a material that can improve the thermal environment in summer. The performance of the material in winter and its form of opening surface are secondary objectives.

3.3 Pareto optimal solutions

Figure 6 shows the Pareto optimal solutions. The color scale in this figure represents the F_{Form} evaluation value. The reflective performances in summer and winter clearly indicated a trade-off relationship. Focusing on the relationship between the summer reflective performance and the form of the opening surface, individuals with higher F_{Summer} values tended to exhibit higher F_{Form} values in Cases 1 and 2. In addition, summer and winter performances are in the relationship of trade-off. Meanwhile, in Case 3, individuals with low F_{Form} values were superior to those with high F_{Form} values for the reflective performances in both seasons,

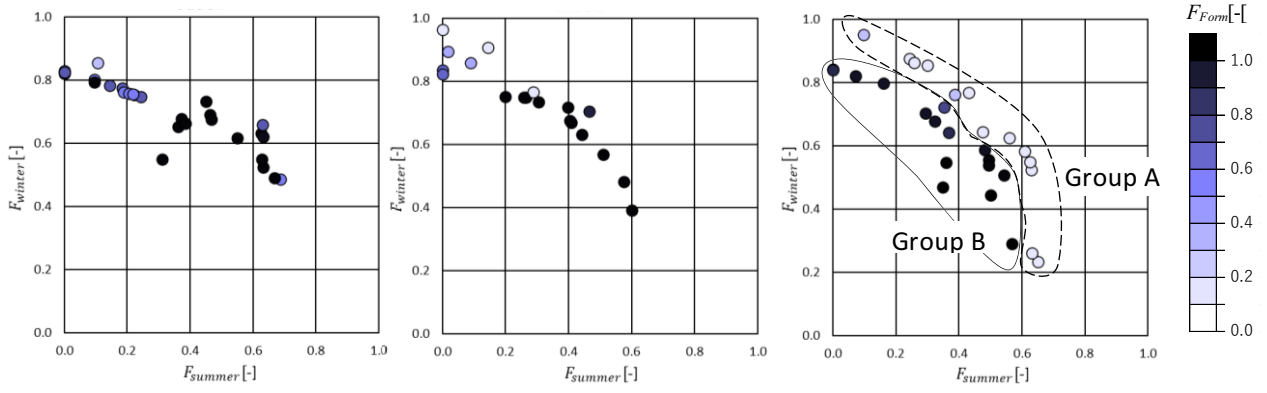

Case 1 (Osaka South) Case 2 (Osaka West) Case 3 (Hong Kong West)

Fig. 6. Pareto Optimal Solutions

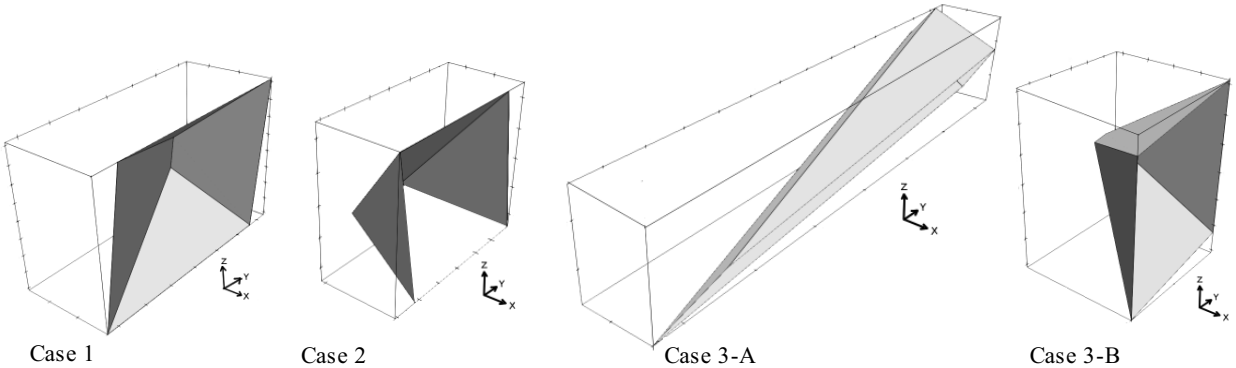

Case 1 Case 2 Case 3-A Case 3-B

Fig. 7. The typical shape

although summer and winter performances are in the relationship of trade-off, same as Cases 1 and 2. The F_{Form} values of Case 3 are divided into two groups more than 0.7 or less than 0.3. It is a peculiar feature. Hence, Individuals in Case 3 with $F_{Form} < 0.3$ were classified as group A and those with $F_{Form} > 0.7$ as group B

3.4 Effects of direction and city of installation on optimal solutions

In this section, we focus on the solutions with high F_{Summer} values (more than 0.5). In each case, the shape difference between individuals with high F_{Summer} values was insignificant. The typical shapes for each case are shown in Fig. 7. In terms of the summer reflective performance, the shapes of Cases 1, 2, 3-A, and 3-B ranked third, second, fourth, and eighth (second within group B), respectively. Figure 8 shows the reflection properties of the individuals in Fig. 7, i.e., the (a) absorption, (b) upward reflectance, and (c) elevation angle of the primary reflection vector. (c) is described in the next section. The horizontal axis in Fig. 8 indicates the azimuth of the light source, and the vertical axis indicates the altitude. As an example, light irradiates the surfaces from the normal direction when the values of both the azimuth and altitude are set to 0° in Case 1. The

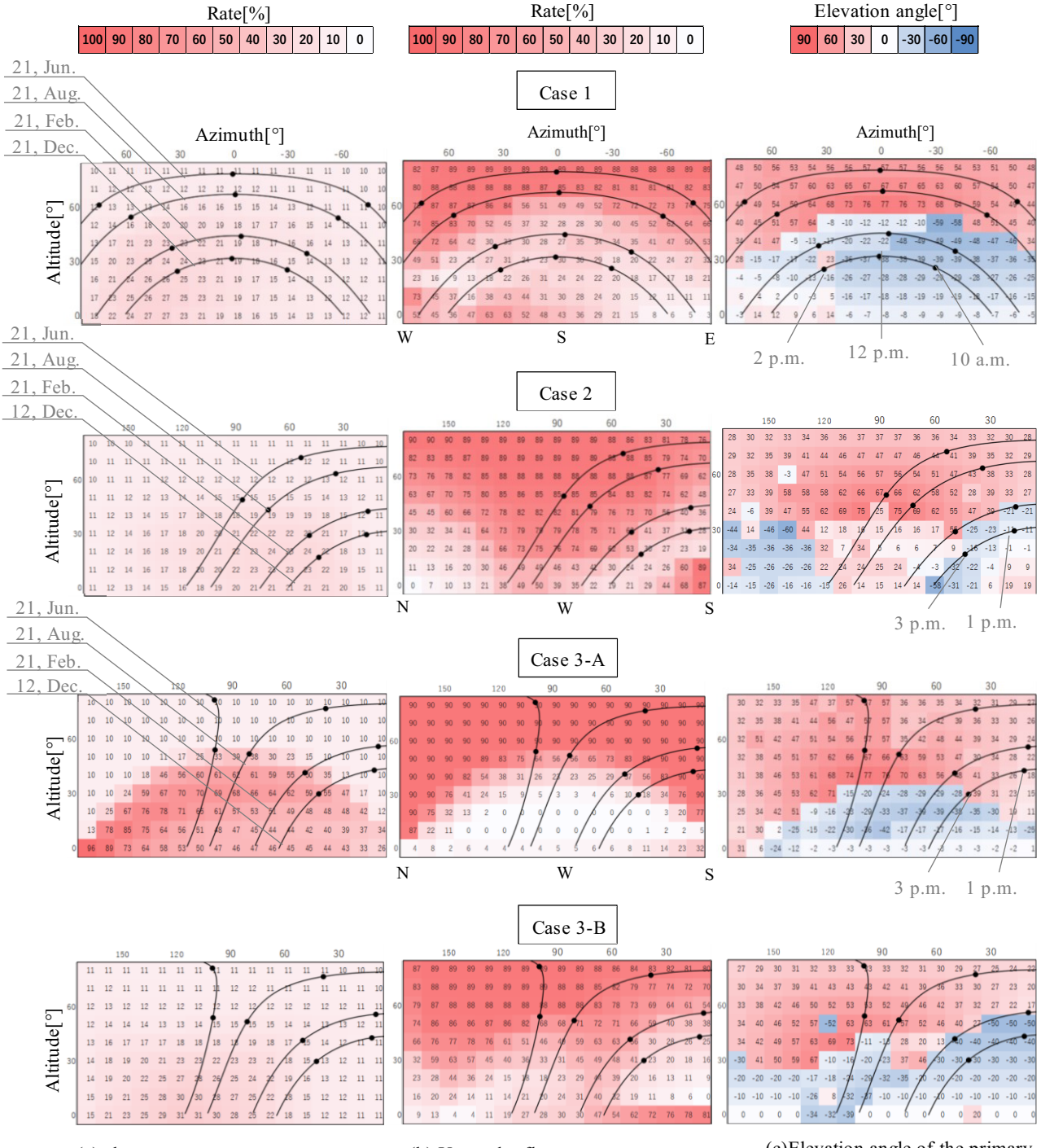

(a) absorptance (b) Upward reflectance (c)Elevation angle of the primary reflection vector

Fig. 8. Reflective properties

same conditions are observed when the values are set to 90° azimuth and 0° altitude in Cases 2 and 3, respectively. The sun paths of the target dates are shown as well. The absorptances of Cases 1, 2, and 3-B were 10%–30% for any incident angle. Furthermore, these cases exhibited similar upward reflectance rates and primary reflection vectors at incident angles around the sun paths. From noon to 3 p.m., the upward reflectance was high in summer but low in winter. The individuals with high F_{Summer} and F_{Form} values exhibited similar reflection properties over the range of incident angles around the sun path, regardless of the installation direction or city. By contrast, case 3-A, with a significantly lower F_{Form}, showed exceptional results. Before 3 p.m., Case 3-A showed strong upward reflectance and low absorption in winter. However, the absorption increased significantly to more than 50% at approximately 3 p.m., which is the target time for Case 3. Hence, the F_{winter} value of Case 3-A became an intermediate value. Case 3-A is considered to be overestimated and an inappropriate solution owing to inadequate target times.

3.5 Determinant of summer reflective performance

This section describes the reflection properties in summer on the basis of the reflection trajectories in a prism. Solar radiation resulted in several trajectories inside the prism and was finally emitted from the prism with different reflection vectors. The reflection vector with the highest energy intensity was named "primary reflection vector," as shown in Fig. 8 (c). Based on the figure, the primary reflection vectors of the individuals were upward from noon to 3 p.m. in summer. This was similarly observed for the other individuals with high F_{Summer} values, except for the two individuals in Case 1. This was attributable to the one-time reflection. In addition, as shown in Fig. 9, the normal vectors of the surface element where solar radiation reached first were similar in each case study. This is an important determinant of the summer reflective performance. The azimuth of the normal was approximately similar to that of the installation surface. The elevation angles were approximately 70° and 60° for the installations in the south and west, respectively, which serve as important guidelines for an optimum design.

4 Conclusion

An optimal design method for near-infrared rays retro-reflective materials installed on the exterior surfaces of buildings was proposed using a MOGA coupled with numerical analysis based on the ray tracing method. In addition, the effect of the installation direction or city on the optimal designs was investigated via a parametric study. The conclusions were as follows:

1) Pareto optimal solutions for the three design goals were obtained for each study case using the proposed method.
2) As a common feature of surface shapes with high summer reflective performance, most of solar radiation hit one of the surface elements of prism only once and reflected upward in summer. Therefore, the normal vector of the surface element where solar radiation reached first suggests an important determinant of the summer reflective performance. In the cases of Osaka and Hong Kong, the elevation angles of the normal vectors were approximately 70° and 60° for the installations in the south and west, respectively.
3) In Osaka, approximately square shapes were indicated as the opening surfaces of the optimal solutions. The installation direction did not significantly affect the optimal shapes.
4) In Hong Kong, some flat horizontal shapes were indicated in Pareto optimal solutions. The optimal designs are considered to depend on the installation city.

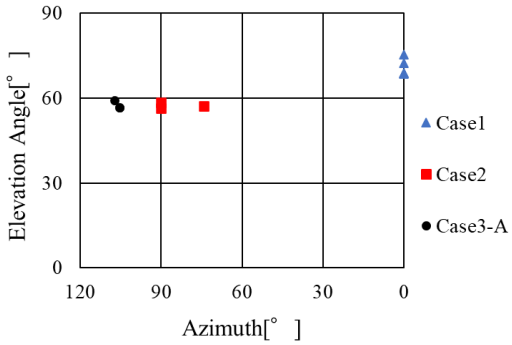

Fig. 9. The normal vector of he primary reflection vector

The following are topics for future study.

1) In Case 3, the target times were considered to be insufficient. Further consideration of the appropriate target times is required to construct a stable system. Using an appropriate analysis time may give a different view of the effect on the city of installation.
2) Since the individuals with high F_{Summer} in cases 1 and 2 had similar prism shapes, the installation direction was considered to have little effect. However, further analysis revealed that the normal vector of the surface element where solar radiation reached first has a difference of approximately 10° depending on the installation direction. Further investigation is needed to determine whether it is a significant difference or not.

References

1. F. Rossi, A. L. Pisello, A. Nicolini, M. Filipponi, M. Palombo, *Analysis of retroreflective surfaces for urban heat island mitigation: a new analytical model*, Applied energy, 114 (2014)
2. S. Yoshida, A. Mochida: *Evaluation of effects of windows installed with near-infrared rays retro-reflective film on thermal environment in outdoor spaces using CFD analysis coupled with radiant computation*, Building Simulation, 11-5 (2018)

3. F. Rossi, B. Castellani, A.a Presciutti, E. Morini, M. Filipponi, A. Nicolini, M. Santamourisc; *Retroreflective façades for urban heat island mitigation: Experimental investigation and energy evaluations*, Applied Energy, 45 (2015)
4. K. Furubayashi, M. Nishioka, and M. Nabeshima, *Reducing Effect of Downward Reflected Solar Radiation from Folded Plate Wall*, Transactions of the Society of Heating, Air-conditioning and Sanitary Engineers of Japan, 42-247 (2017), (written in Japanese)
5. T. Uchiike, Y. Oyama, K. Umeda, H. Kubota, M, Oguro, H. Sasaki, C. Ishikawa, K. Sakai, M. Nishioka, *Development of directive control reflector for countermeasures to urban heat island: Part 2 Effects of diffuse reflectors*, Summaries of technical papers of Annual Meeting Architectural Institute of Japan. D-1 (2010) (written in Japanese)
6. M. Nishioka, K. Sakai, C. Ishikawa, Y. Oyama, M, Oguro, T. Uchiike, Y. Namatame, H. Kubota, H. Sasaki, *Development of directive control reflector for countermeasures to urban heat island: Part4 Bidirectional reflectance for tile reflector prototype*, Summaries of technical papers of Annual Meeting Architectural Institute of Japan. D-1 (2011) (written in Japanese)
7. H. Tamaki, M. Mori and M. Araki, *Generation of a set of Pareto-optimal solutions by genetic algorithms*, Trans of the Society of Instrument and Control Engineers, 31-8 (1195) (written in Japanese)